Supplementary Information

Graphene Wrapping as a Protective Clamping Layer Anchored to Carbon Nanofibers Encapsulating Si Nanoparticles for a Li-Ion Battery Anode

*Jungwoo Shin, Kyusung Park, Won-Hee Ryu, Ji-Won Jung and Il-Doo Kim**

Synthesis and optimization of CNFs/SiNPs

To determine the optimal SiNPs concentration within CNFs, we carried out electrospinning with multiple concentrations of SiNPs. Polymeric fibers including SiNPs with different weights of 0.1 g (Fig. S1a), 0.3 g (Fig. S1b), and 0.5 g (Fig. S1c) were synthesized. Fig. S1d-1f shows SEM images of carbon nanofibers encapsulating SiNPs (CNFs/SiNPs) after carbonization, with SiNPs concentrations of 0.1 g, 0.3 g, and 0.5 g, respectively. There was little morphological change of each fiber during calcination. XRD spectra in Fig. S2 reveal that CNFs/SiNPs exhibited sharp peaks corresponded to Si crystals. Since SiNPs in the CNFs/SiNPs (0.5 g) sample were extremely aggregated and extruded out of CNFs, CNFs/SiNPs (0.3 g) were chosen as an optimum condition providing the maximum SiNPs composition without severe aggregation.

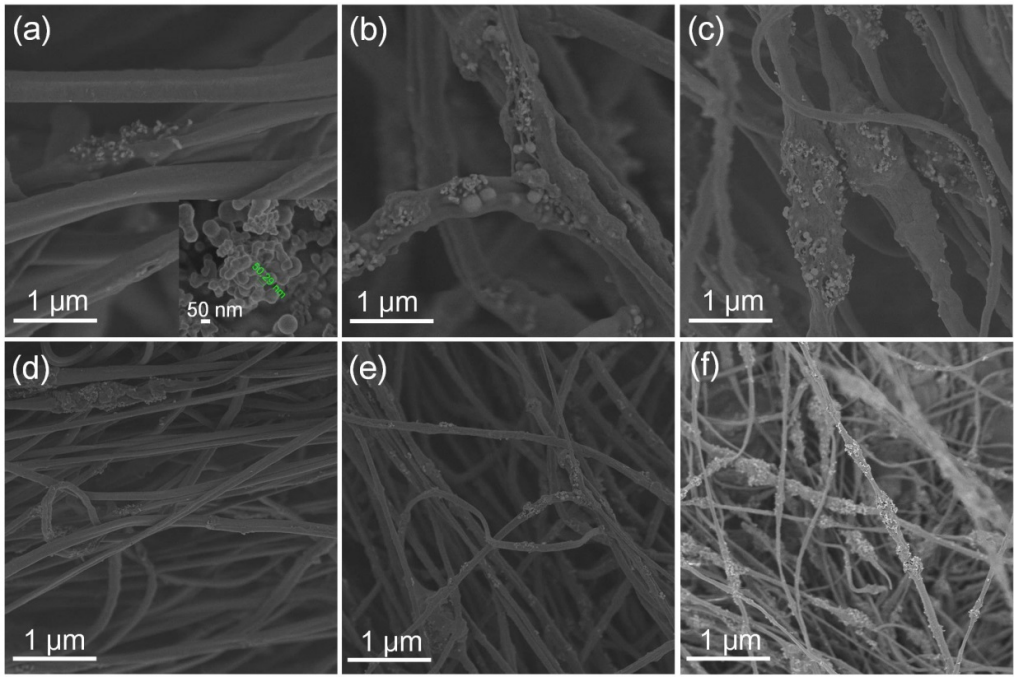

Fig. S1 SEM image of polymeric-fibers/SiNPs with SiNPs weights of (a) 0.1 g, (b) 0.3g and (c) 0.5 g; SEM image of carbonized CNFs/SiNPs with SiNPs concentrations of (a) 0.1 g, (b) 0.3g and (c) 0.5 g.

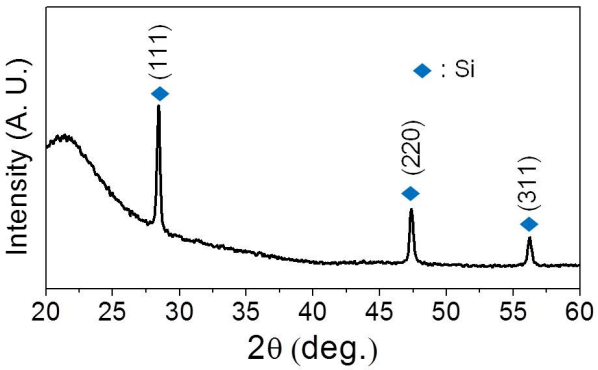

Fig. S2 XRD pattern of CNFs/SiNPs.

The CNFs/SiNPs were functionalized with APS, and the graphene assembly was carried out by dispersing functionalized CNFs/SiNPs and GO in an aqueous solution (pH 4). After mild stirring of 1 h, 1 ml of hydrazine monohydrate was added to the solution and heated to 80 ^{o}C. After 3h stirring this suspension is cooled to room temperature. As shown in Fig. S3, rGO wrapped CNFs/SiNPs (CNFs/SiNPs@rGO) slowly segregated from the aqueous solution due to the change in hydrophobicity of the composite. Separated CNFs/SiNPs@rGO was then collected.

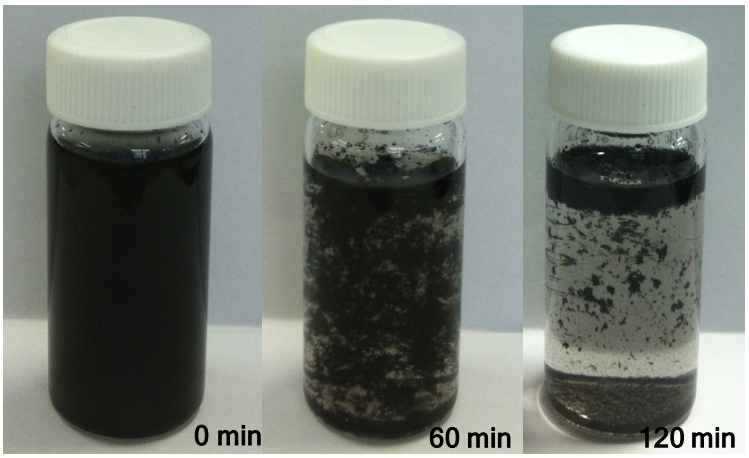

Fig. S3 Photographs of CNFs/SiNPs@rGO after hydrazine reduction followed by cooling at room temperature.

To verify the graphene wrapping conformational effect on electrochemical performance, we observed and carried out rate capability tests of CNFs/SiNPs@rGO with different GO concentrations: (a) 0.13 mg ml^{-1}, (b) 0.26 mg ml^{-1}, and (c) 0.4 mg ml^{-1}. Fig. S4 shows that the conformation of CNFs/SiNPs@rGO is highly relevant to the concentration of GO solution used in the wrapping process. Fig. S4a-c shows schematic illustrations of CNFs/SiNPs@rGO with respect to different GO concentrations: (a) GO starts to wrap around CNFs/SiNPs, (b) GO fully covers CNFs/SiNPs, and (c) GO accumulates on fully wrapped CNFs/SiNPs. At a low GO concentration, chemical grafting between GO and CNFs/SiNPs takes place on the limited surface (Fig. S4d). In this case, it is difficult to observe a single fiber fully covered with graphene, but graphene (yellow arrow) was draped around a single fiber (left) or two fibers (middle). Nonetheless, every single graphene sheet was sandwiched between the fibers without stacking or agglomeration, as shown in the side cut view (right, inset). Note that the graphene wrapping might appear to be detached from CNFs/SiNPs due to the large fraction force during cutting. As the GO concentration reaches the critical concentration where every single fiber is fully wrapped, redundant graphene sheets start to adhere to the outermost surface of graphene wrapping (Fig. S4e). These graphene overcoats span across multiple fibers with a weak Van der Waals force, and are stretched tightly between the fibers on account of the high surface tension (left, middle). The side cut view reveals that the individual fibers were fully covered with a thin, flexible graphene wrapping with distinguishable graphene overcoats (right). In Fig. S4f, accumulation of such graphene overcoats resulted in substantial graphene stacking on the outermost CNFs/SiNPs surface (left, middle). These graphene layers resulted in thickened graphene stacking (right, inset).

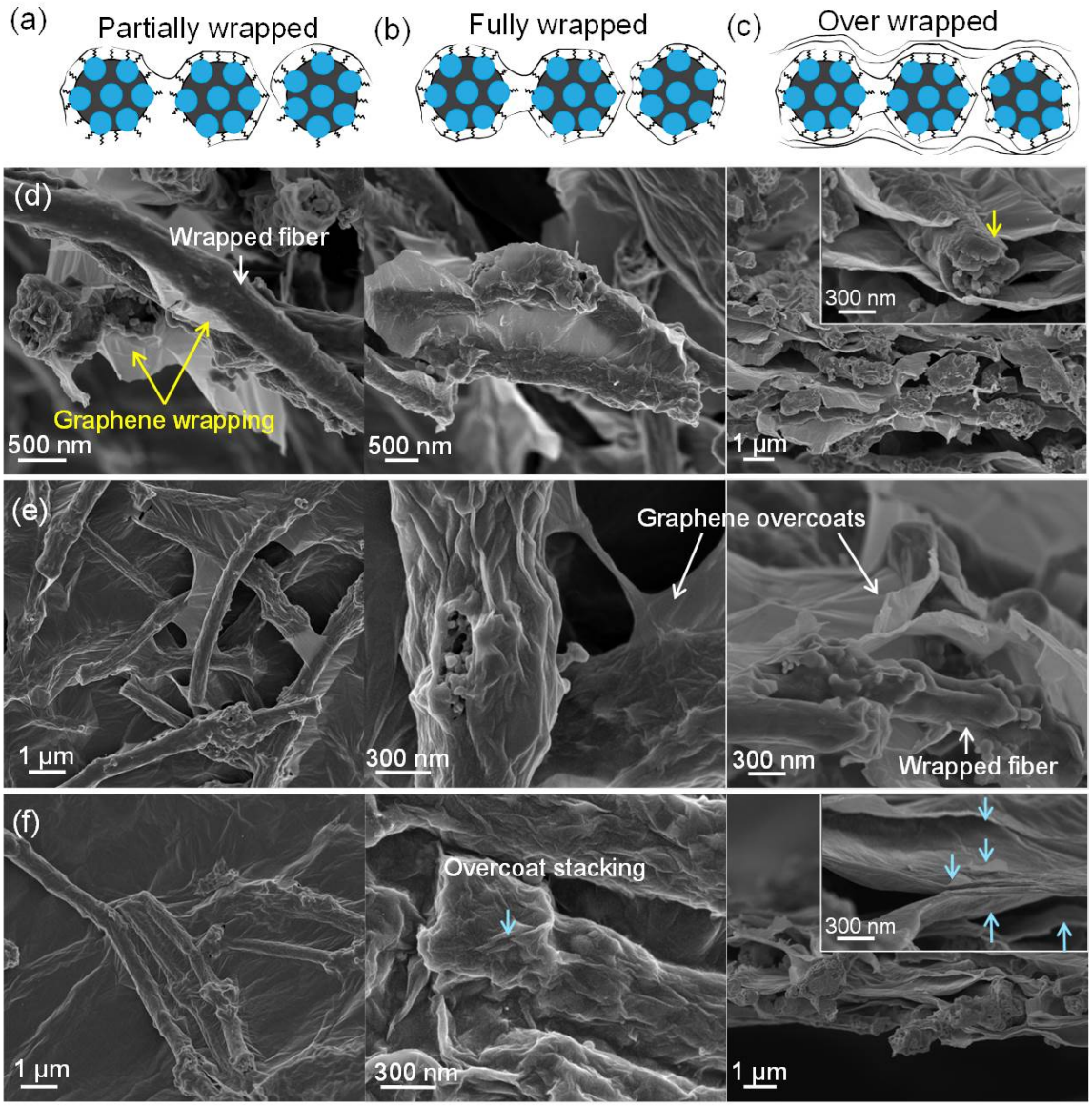

Fig. S4 Schematic illustration of CNFs/SiNPs@rGO at each phase of wrapping step corresponding to (a) partial (0.13 mg ml^{-1}), (b) full (0.26 mg ml^{-1}) and (c) excessive (0.4 mg ml^{-1}); SEM images of CNFs/SiNPs@rGO for (d) partial, (e) full and (f) excessive wrapping with different magnifications.

The characteristic wrapping conformation, however, did not appear when GO assembly was carried out without APS modification. Due to the absence of positive charges on the CNFs surface but negative charges arising from hydroxyl groups in SiNPs and carboxylic acid groups in CNFs, GO could not simply cling to the CNFs/SiNPs curvature due to the strong electrostatic repulsion even at low GO concentration, as shown in Fig. S5a. Therefore, the rGO was segregated and transformed into a thick graphite-like plate, as illustrated in Fig. S5b, where the GO concentration is equivalent to the fully wrapped condition for functionalized CNFs/SiNPs@rGO. Further addition of GO not only resulted in the thick stacks of graphite flakes but also rGO-aggregated-balls, as shown in Fig. S5c. Fig. S5d-f shows SEM images of rGO aggregation behavior corresponding each illustration above.

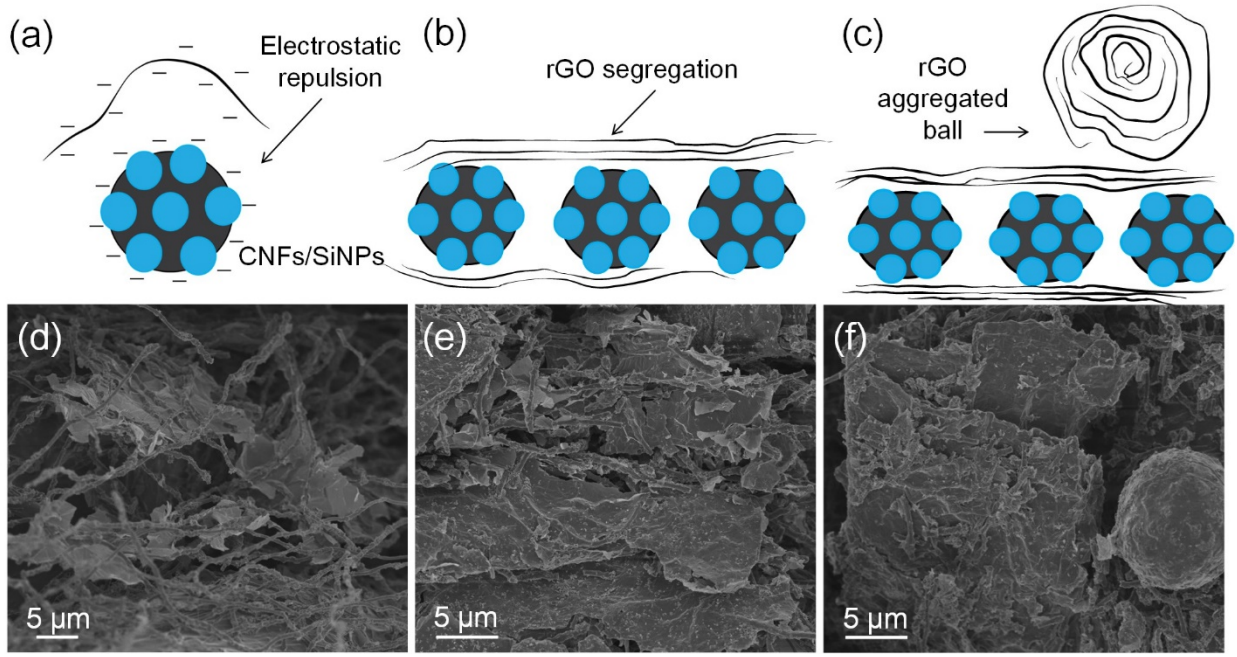

Fig. S5 Schematic illustration of non-functionalized CNFs/SiNPs@rGO at each phase of graphene aggregation with three different GO concentrations equivalent to those in Fig. S4: (a) partial, (b) full, and (c) excessive. (d), (e) and (f) are SEM images of non-functionalized CNFs/SiNPs@rGO corresponding to the GO conditions illustrated in (a), (b) and (c), respectively.

Fig. S6 shows the electrochemical performance of each CNFs/SiNPs@rGO with different GO concentrations, as illustrated in Fig. S4a-c. Since partially wrapped CNFs/SiNPs@rGO cannot isolate active materials from the electrolyte and accommodate volume expansion of SiNPs, it exhibited severe capacity fading after the rate-varying test. Fully wrapped and over-wrapped CNFs/SiNPs@rGO showed almost flat capacity retention after cycling after the rate-varying test and demonstrated greatly improved high-rate performance.

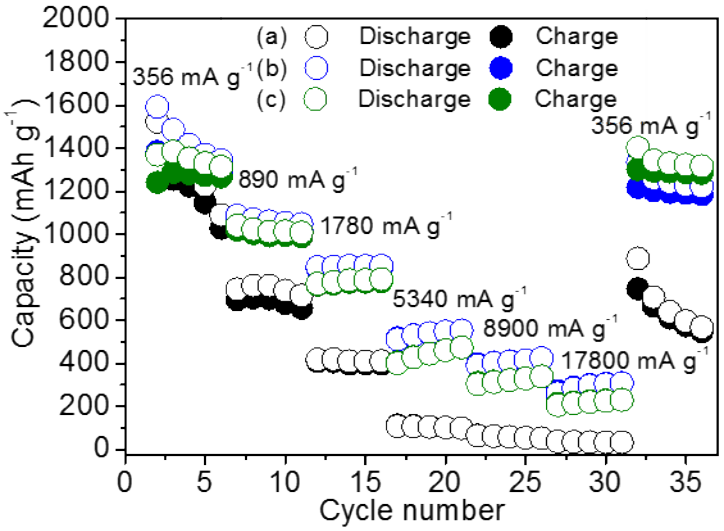

Fig. S6 Electrochemical performance of partial, full and over-wrapped CNFs/SiNPs@rGO operated at 356 mA g^{-1} to 17800 mA g^{-1} at each wrapping step.

For EIS data evaluations, the equivalent circuit model in Fig. S7 is used. Fig. S8 shows Nyquist plots of CNFs/SiNPs and CNFs/SiNPs@rGO after the first discharge, and Table S1 presents the corresponding impedance resistance values.

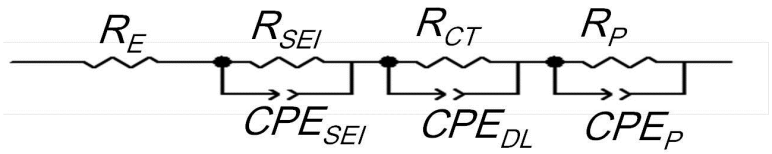

Fig. S7 The EIS equivalent circuit model of CNFs/SiNPs and CNFs/SiNPs@rGO.

Fig. S8 and Table S1 show the Nyquist plots of CNFs/SiNPs and CNFs/SiNPs@rGO after the first discharge. The size of semicircles and the fitted value of both samples are larger than those of cycled samples. Although the thickness of SEI layer increases after cycling, ion pathway can be developed so that Li ion diffusion length is reduced and Li ion transfer kinetics becomes faster as lithiation/delithiation repeated. During many electrochemical cycles, with several breakage and recovery of SEI layers, it can form dense and stable phase which reduces effective surface resistance compared to that of the first discharged cell.

Fully developed cell whose active materials are reversibly lithiated and delithiated so that the coulombic efficiency reaches to almost 100% and first discharged cell whose coulombic efficiency is way below 100%, may exhibit differences in chemical property of chemical property and diffusivity of Li ions in SEI layer.

Another fact is that the formation of SEI layer is strongly affected by the presence of native layer for Si anode. When the native layer is present, the SEI resistance is very high. Once the native layer is completely destroyed during cycling and Si surface is covered with stable SEI layer, the interphase resistance abruptly decreased so that the fully reacted Si anodes can show less SEI resistances.

Here, the differences of SEI resistances and charge transfer resistances between first discharged CNFs/SiNPs and CNFs/SiNPs@rGO indicate the graphene wrapping exhibits better charge transfer process due to the high electric conductivity. As cycle goes, the charge transfer resistance of CNFs/SiNPs is reduced from 168.1 Ω to 133.4 Ω while the charge transfer resistance of CNFs/SiNPs@rGO is reduced from 30.99 Ω to 15.70 Ω. The dramatic charge transfer resistance enhancement of CNFs/SiNPs@rGO indicates its beneficial effect on the quality of Li ion transfer kinetics.

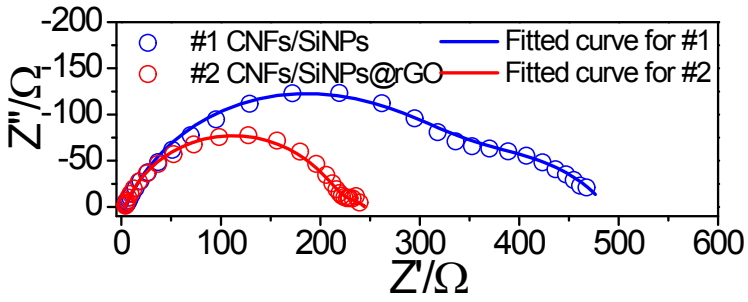

Fig. S8 Nyquist plots of CNFs/SiNPs and CNFs/SiNPs@rGO after first discharge presented with fitted curves.

Table S1 EIS component values calculated from data presented in Fig. S8.

	R_{SEI} (Ω)	R_{CT} (Ω)
SiNPs/CNF	315.8	168.1
SiNPs/CNF@rGO	210.6	30.99